M&C 2017 - International Conference on Mathematics & Computational Methods Applied to Nuclear Science & Engineering, Jeju, Korea, April 16-20, 2017, on USB (2017)

A Multigroup Interpolated Compton Scattering Treatment for the Implicit Monte Carlo Method

Kendra P. Keady*, Terry S. Haut, and Mathew A. Cleveland
LA-UR-17-21303

CCS-2, Los Alamos National Laboratory, P.O. Box 1663, Los Alamos, NM
**keadyk@lanl.gov*

Abstract - *Compton scattering is an important means of energy exchange between radiation and matter in many problems of interest to the astrophysics and high-energy-density physics communities. The Compton scattering kernel is difficult to evaluate numerically because it is a complicated function with boundary layers in frequency, angle, and electron temperature. In this work, we present a new application to produce accurate Compton data libraries for use in thermal radiative transfer codes. Our library makes use of established series approximations to calculate pointwise values of the Compton scattering kernel on a carefully chosen temperature-frequency grid. Numerical integration is then used to obtain multigroup opacities at fixed electron temperature points, which can subsequently be interpolated to obtain opacities at any temperature within the bounds of the library.*

Preliminary results show excellent agreement between the interpolated multigroup method and a previously-implemented explicit sampling routine. In addition, the direct sampling used in the multigroup method is considerably more efficient than the rejection sampling required by the explicit Compton method.

I. INTRODUCTION

Compton scattering involves the inelastic scattering of photons by electrons or other charged particles, and generally dominates photon-matter interactions when the incident photon energy is comparable to the rest mass-energy of an electron (i.e. from tens to several hundred keV). If the colliding free electron has sufficient kinetic energy, the photon can gain energy as a result of the scattering event (a phenomenon referred to as inverse Compton scattering). Thus, to accurately model material energy deposition in a physical system at high temperature, one must account for electron motion when simulating Compton events.

In this work, we present an interpolated multigroup approach to model Compton interactions between photons and relativistic free electrons in thermal radiative transfer simulations. While this paper focuses on the Implicit Monte Carlo (IMC) method, planned future work includes adapting the interpolated multigroup Compton method for use in discrete-ordinates simulations. Our method involves building a library of pointwise Compton Scattering Kernel (CSK) values using a fast numerical scheme originally developed by Kershaw et. al. [1]. Frequency and electron temperature evaluation points are carefully chosen to capture steep boundary-layer variation in the CSK. Tabulated data can then be used to construct multigroup opacities for a given frequency-group structure, which is stored for later use. At each time-step, probability distributions for outgoing photon frequency and scattering angle are calculated using Lagrange interpolation on a subset of electron temperature evaluation points. Because the CSK is (by definition) averaged over a relativistic Maxwellian at the effective electron temperature, electron motion is taken into account without generating an explicit electron realization for each scattering event.

II. BACKGROUND AND METHODOLOGY

The CSK, defined as the Klein-Nishina cross-section averaged over a relativistic Maxwellian electron speed distribution, is given by

$$\sigma_s(\gamma \to \gamma', \xi, \tau) = \frac{N_e r_0^2}{2\gamma\nu} \int f(v) \frac{1}{\lambda} \left\{ 1 + \left[1 - \frac{(1-\xi)}{\lambda^2 D D'} \right]^2 + \frac{(1-\xi)^2 \gamma\gamma'}{\lambda^2 D D'} \right\} \delta\left[\xi - 1 + \lambda\frac{D}{\gamma'} - \lambda\frac{D'}{\gamma} \right] d\boldsymbol{v} \,, \tag{1}$$

$$\boldsymbol{v} \equiv v\Omega \,, \quad D \equiv 1 - \Omega \cdot \frac{\boldsymbol{v}}{c} \,, \quad D' \equiv 1 - \Omega' \cdot \frac{\boldsymbol{v}}{c} \,, \quad \xi \equiv \Omega \cdot \Omega' \,. \tag{2}$$

where N_e is the electron density, $\mathbf{v}$ is the electron velocity vector, and τ is the electron temperature scaled by the electron rest-mass (m_e). The variable λ is the Lorentz factor,

$$\lambda = \frac{1}{\sqrt{1 - v^2/c^2}} \,.$$

Incident and exiting photon frequencies are given by γ and γ', respectively, and are also scaled by the electron rest-mass. The function $f(v)$ is the relativistic Maxwellian speed distribution,

$$f(v) = \frac{\lambda^5 \exp(-\lambda/\tau)}{4\pi\tau c^3 K_2(\tau^{-1})} \,, \tag{3}$$

where K_2 is the modified Bessel function of the second kind. The CSK expression shown in Eq. (1) is a detailed function of frequency, angle, and electron temperature, which complicates attempts to sample this kernel adequately using IMC.

An analog explicit-sampling routine can be used to treat Compton scattering events [2], which we hereafter refer to as the Explicit Compton (EC) method. For each Compton event, the EC method (i) generates a suitable electron using rejection sampling, (ii) boosts the incident photon into the electron rest frame, (iii) samples a frequency and angle for the scattering event in the rest frame, and finally (iv) "un-boosts" the photon back to the lab frame.

While this sampling scheme is accurate, it is also inherently noisy. Because the CSK is such a complicated function, energy deposition can vary substantially between subsequent Compton events (even if the incident photons have similar attributes). In practical calculations, it is not generally feasible to simulate enough EC scatters to adequately sample the full phase space of the CSK.

This observation led us to consider an alternate scattering treatment, wherein the angle and energy distributions for Compton scattering are interpolated at the beginning of each time-step from multigroup data in an existing library. We refer to this as the multigroup Interpolated Compton (IC) method. This treatment, in theory, should benefit the IMC calculation in a number of ways. First, by interpolating the electron-speed-averaged Compton scattering opacities at the beginning of each time-step, we avoid the use of rejection sampling during the simulation. Instead, we directly sample an outgoing frequency group and scattering angle from the multigroup distribution functions, which is more efficient than generating an electron realization for each Compton scatter.

In this work, we also use CSK data to calculate an average outgoing frequency $\bar{\gamma}'$ for each $(g \to g')$ combination and scattering bin (${\bar{\gamma}'}^{l}_{g\to g'}$, where l is an angular index). This significantly reduces noise in the outgoing frequency distribution (relative to the EC method). If further investigation reveals a need for additional noise suppression, it is straightforward to average the existing $\bar{\gamma}'$ values over angle. This would yield a single average outgoing frequency for each $g \to g'$ combination (${\bar{\gamma}'}_{g\to g'}$).

Finally, we can (in theory) use knowledge of the scattering distribution to inform the photon frequency group structure of the problem.

Two numerical methods are used to evaluate the pointwise CSK values which form the basis of our multigroup libraries. If the electron temperature is reasonably high ($>\sim 5$ keV), we use the exact expression given as Eq. (38a) in Kershaw et. al. [1], truncated to $n = 15$. If, however, the electron temperature is low or ξ is very close to unity, this expansion is highly susceptible to loss of accuracy; thus, in the low-temperature regime, we employ the asymptotic series given as (16a) in Kershaw et. al. [1]. We note that the multigroup IC libraries are currently only used to supply shape functions for photon scattering angle and outgoing frequency group, while the total Compton cross section in each frequency group is retrieved from opacity data tables (or input manually by the user).

To obtain usable multigroup scattering opacities from the pointwise data, we integrate over a specified frequency group structure in γ and γ' to obtain multigroup scattering matrices. This step is carried out "offline" to avoid undue increase in simulation time, with the resulting multigroup library retained for re-use (these multigroup libraries are reasonably sized, averaging 10-20 MB per electron temperature evaluation point). e interpolate between electron temperature tables at each time-step to obtain approximate multigroup CSK opacities for each spatial cell. If the incident photon frequency is outside the bounds of the multigroup data library, we simply revert to the existing EC method.

In the following sections we briefly discuss our pointwise library generation method. The resulting pointwise libraries are designed to enable accurate interpolation of the CSK over a broad range of frequencies, scattering angles, and electron temperatures.

1. Pointwise library generation

A. Electron temperature evaluation points

Variation in the CSK with respect to electron temperature is dominated by the relativistic Maxwellian distribution term (specifically, the factor of $\exp(-\lambda/\tau)$ and the Bessel function, $K_2(\tau^{-1})$). This exponential term decreases very rapidly as $\tau \to 0$, which can lead to underflow error at very low electron temperatures. The Bessel function $K_2(\tau^{-1})$ also decreases rapidly with decreasing electron temperature. These two terms render the CSK very sensitive to small changes in τ as $\tau \to 0$. Far away from $\tau = 0$, the electron temperature variation of the CSK is relatively smooth, and can be interpolated accurately using a low-order Lagrange polynomial with widely-spaced evaluation points.

To capture the shape of the boundary layer as $\tau \to 0$, we use a double-exponential quadrature rule to "bunch" electron temperature breakpoints in the steeply-varying region. Care is taken to evaluate the exponential and Bessel function terms using special scaling relations in the low-temperature limit, such that their ratio does not suffer catastrophic loss of accuracy.

B. Frequency mapping and interpolation

The variation of the CSK with respect to incident and outgoing frequency is marked by two interior boundary layers on $\gamma, \gamma' \in (0, \infty)$. In addition, there are boundary layers as $\gamma \to 0$ and $\gamma' \to 0$ which represent the physical bounds of the Compton scattering process (because photons cannot scatter to or from negative frequencies). To accurately capture frequency trends in the CSK, we divide the frequency space into three interpolation regions defined by the boundary layers in γ and γ'. Specifically, the interior boundary layers in (γ, γ') are given by

$$\gamma' = \frac{\gamma}{(2\gamma + 1)} \tag{4}$$

and

$$\gamma' = \gamma \, . \tag{5}$$

Next, we transform each of the interpolation regions from $(\gamma, \gamma') \to (x, y)$, where x and y define a unit square. This is done using the following mapping functions:

$$\gamma' < \frac{\gamma}{(2\gamma + 1)} :$$

$$
\begin{aligned}
x &= \gamma \,, \\
y &= 1 - \frac{2\gamma\gamma'}{2\gamma + 1} \,, \\
\frac{\gamma}{(2\gamma+1)} < \gamma' < \gamma : & \\
x &= \gamma \,, \\
y &= 1 - \frac{\gamma - \gamma'}{2\gamma\gamma'} \,, \\
\gamma' > \gamma : & \\
x &= \gamma \,, \\
y &= (\gamma' - \gamma) \,. \qquad (6)
\end{aligned}
$$

A double-exponential quadrature rule is applied to define interpolation subregions in (x, y) space; this generates break points that are "stacked" against the boundaries of the unit square. Local evaluation points are generated in each breakpoint region using a 1-D Gauss-Legendre quadrature rule. Once this process is carried out, two-dimensional Lagrange interpolation can be used to estimate the value of the CSK at any (γ, γ') point interior to breakpoint region (i, j) (where i and j are the breakpoint region indices in x and y, respectively). This method of choosing frequency evaluation points ensures that the original CSK boundary layers in (γ, γ') are adequately captured in (x, y)-space.

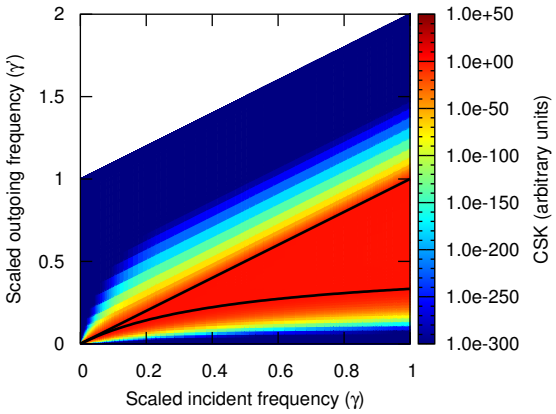

Fig. 1. CSK variation at $T_m \approx 0.345$ keV, with interior boundary layers shown in black.

Figure 1 plots variation in the zeroth Legendre moment of the CSK with respect to γ and γ', evaluated at $\tau \approx 0.345$ keV (we note that the values shown in Figure 1 exclude scaling constants). Color data in Figure 1 is calculated using the average of CSK evaluations at the four corner nodes. This figure captures the drastic variation in CSK magnitude with frequency, with changes of over three hundred orders of magnitude as one traces a vertical (constant-γ) line across the figure. Interior boundary layers are plotted in black; these lines divide the three interpolation regions, each of which is mapped to a unit square.

In Figure 2, we present the same zeroth-moment CSK data after the unit square mapping. We also include dots to indicate CSK evaluation points in (x, y) space. As previously described, the evaluation points are chosen to bunch against the boundary layers at the outer edges of the unit square.

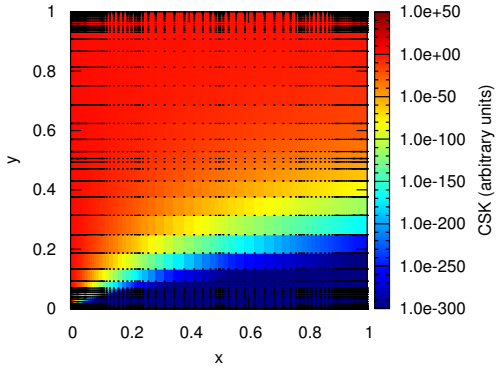

(a) Bottom region

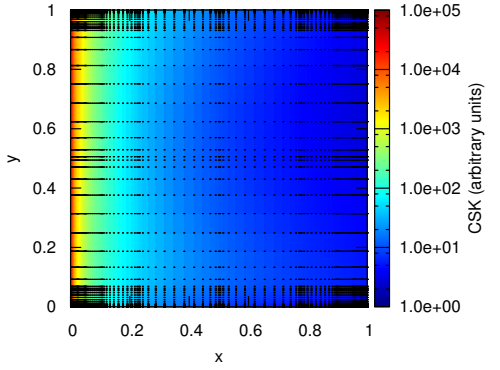

(b) Middle region

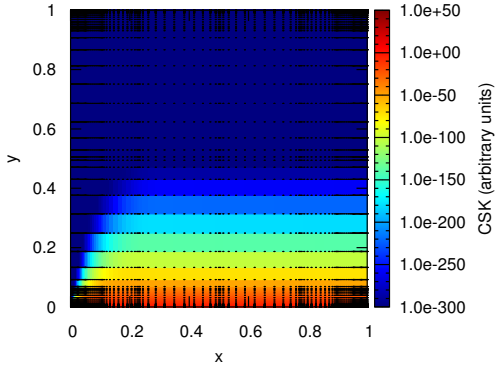

(c) Top region

Fig. 2. CSK data remapped to unit square by boundary layer region

Now that the strategy for pointwise library generation has been outlined, we discuss how this pointwise data is used to build multigroup opacities for a given frequency group structure.

2. Multigroup library generation

We calculate our group-to-group scattering opacities using the following expression,

$$\sigma^l_{s,g\to g'}(\tau) = \int_{\gamma_{g',min}}^{\gamma_{g',max}} \int_{\gamma_{g,min}}^{\gamma_{g,max}} \sigma^l_s(\gamma \to \gamma', \tau) I(\gamma, \tau) d\gamma d\gamma' \ , \quad (7)$$

where g is the incoming frequency group, g' is the outgoing frequency group, and $I(\gamma)$ is a spectral weighting function (our application currently provides flat, Planckian, and Wien weighting functions). The angular index, l, can indicate either the l^{th} Legendre moment or the l^{th} explicit angular evaluation point, depending on library type (results for both angular treatments can be found in Section III.1.).

To generate multigroup opacities at an electron temperature evaluation point in the given pointwise library, we numerically integrate the pointwise data over incoming and outgoing frequency. Because frequency groups may span interior boundary layers, special checks are implemented to ensure a sufficient number of points are generated to adequately resolve variation in the CSK near the boundary layer. The weighting function $I(\gamma)$ is included in the numerical integration over γ.

In addition to frequency mapping information, the pointwise library also contains a list of electron temperature breakpoints and the number of local evaluation points per region. This information allows for the construction of a Lagrange interpolating polynomial in each electron temperature breakpoint region. Thus, once multigroup data is calculated for all electron temperature points in the pointwise library, multigroup opacities can be obtained via Lagrange interpolation for any electron temperature within the bounds of the library.

Our initial implementation of the multigroup IC method placed outgoing photons randomly in the sampled frequency bin for the subsequent energy deposition tally. In essence, this treatment assumes that the average outgoing frequency is roughly equal to the bin center. However, preliminary energy deposition results indicate that this assumption is generally invalid, especially when $g \neq g'$ (see Table I). To improve the accuracy of IC, we now calculate an additional $\bar{\gamma}'$ value for each $(g \to g', l)$ data point. This is done using a numerically-integrated approximation of the exact expression for ${\bar{\gamma}'}^l_{g\to g'}$ given by:

$${\bar{\gamma}'}^l_{g\to g'}(\tau) = \frac{\int_{\gamma_{g',min}}^{\gamma_{g',max}} \gamma' \int_{\gamma_{g,min}}^{\gamma_{g,max}} \sigma^l_s(\gamma \to \gamma', \tau) I(\gamma, \tau) d\gamma d\gamma'}{\sigma^l_{s,g\to g'}(\tau)} \ ,$$

where $\sigma^l_{s,g\to g'}(\tau)$ is given by Eq. (7).

In the improved implementation, the outgoing frequency is uniquely determined once the frequency group and scattering bin are chosen. In the future, we may transition to a single $\bar{\gamma}'$ for each $g \to g'$ combination (averaged over all scattering angles). This would simplify the outgoing frequency spectrum considerably, which may also aid in suppressing noise in the material energy deposition tally.

A. Known issues with multigroup data

The Lagrange interpolation procedure used to generate additional CSK estimates for γ/γ' integration is generally accurate, provided the number of evaluations per breakpoint region in the pointwise library is large; however, the CSK can still exhibit very steeply-varying behavior within a single breakpoint region, which leads to a significant loss of interpolation accuracy. This issue can generally be assuaged by regenerating the pointwise library with an increased number of breakpoint regions and/or local interpolation points. We stress that even when the number of pointwise evaluations is large, the Lagrange interpolation procedure does not guarantee positivity. This is true even when the local evaluation points are non-negative (as is the case with our pointwise CSK libraries). In extreme cases, this phenomenon produces negative multigroup scattering opacities (which are non-physical).

In addition, use of a Legendre moment treatment in angle is highly inaccurate for certain frequency group in/out combinations. This is especially visible in distribution functions for downscattered photons, which approach an exponential shape and are nearly zero over a large portion of the angular domain. Because the Legendre moment method cannot adequately capture this steeply-varying angular shape, the Legendre IC method sometimes causes photons to scatter in directions that are not physically possible.

Finally, we point out that our preliminary Planck-weighted multigroup data libraries assume full equilibrium between radiation and matter; that is, they calculate the spectral weighting function for the radiation using the material temperature (T_m). Extending our application to treat the case where $T_m \neq T_r$ is straightforward; however, it greatly increases the total amount of data that must be stored to build a multigroup library, and introduces yet another variable that requires interpolation. As a result, we restrict the discussion in this paper to problems where $T_m \approx T_r$.

III. NUMERICAL RESULTS

In this section, we compare single-scatter numerical results from our new multigroup IC method to the existing explicit method in Jayenne. To verify that our data library and sampling procedures are implemented correctly, we first investigate outgoing frequency group and angular distributions. This comparison is performed for both flat-weighted and Planck-weighted IC opacity libraries. In the flat-weighted case, we present results for both explicit and Legendre angular treatments.

Finally, we compare average outgoing frequency distributions for IC and EC using the Planck-weighted library. These distributions demonstrate the ability of the IC method to produce smooth outgoing frequency distributions. This, in turn, decreases noise in material energy deposition distributions, which are directly related to outgoing photon frequency.

The distributions shown in this section all correspond to a material temperature of roughly 0.345 keV, which coincides with one of the temperature evaluation points in our pointwise library. Thus, we have not yet examined the accuracy of the Lagrange interpolation procedure in electron temperature; however, because the τ-variation of the CSK is generally smoother than the frequency variation, we expect interpolation in electron temperature to introduce negligible additional error.

The flat- and Planck-weighted multigroup IC libraries

used in this work were generated from two existing pointwise libraries with different interpolation grids. As previously described, we employ Lagrange interpolation between pointwise frequency evaluations as necessary to form the multigroup opacities.

1. Flat-weighted library

The flat-weighted multigroup libraries compared here use a thirty frequency-group structure, ranging from a lower bound at $\nu_0 = 0.75$ keV to an upper bound at $\nu_{max} = 30$ keV. Group 1 is of width $\Delta\nu = 0.25$ keV, while groups 2 through 30 are of width $\Delta\nu = 1.0$ keV. Because these libraries use a uniform spectral weighting function across all frequency groups, they makes no assumption about the effective radiation temperature (T_r). The multigroup library with Legendre moment angular treatment is truncated to P_{50}, while the library with explicit angular treatment uses 200 equally-spaced CSK evaluations in ξ.

The figures in this section were generated using 5e6 scattering events per simulation. To provide a fair comparison between IC and EC, we sourced particles uniformly within frequency group 23 (thus approximating a flat spectral weighting function across the group).

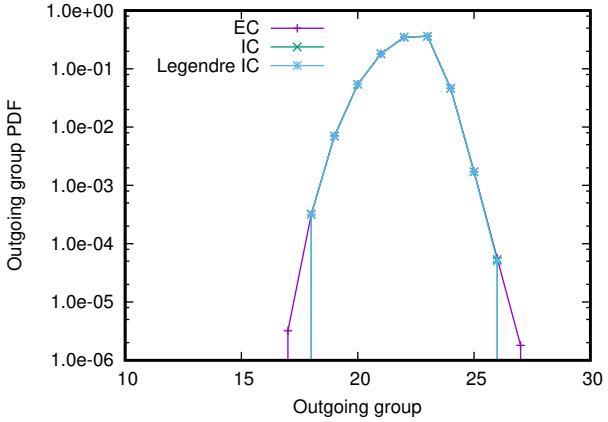

Fig. 3. Single-scatter outgoing g' distribution function, $g = 23$.

Figure 3 plots the outgoing frequency group distribution for EC, IC with an explicit angular treatment (labeled "IC" in the figure), and IC with a P_{50} Legendre moment angular treatment (labeled "Legendre IC"). We observe excellent agreement between the three curves for outgoing groups between 18 and 26; however, the IC and Legendre IC PDFs drop to zero in outgoing groups 17 and 27, while a small fraction of EC events scatter into these groups. This phenomenon is an artifact of the IC interpolation scheme; when the true group-to-group scattering probability is very small (but non-zero), Lagrange polynomial interpolation can produce non-physical (negative or oscillating) scattering opacities (see Section II.2.A.). This is the case for outgoing IC groups 17 and 27; thus, we set the PDF to zero in these frequency bins.

Next, Figure 4 compares EC, IC, and Legendre IC scattering angle distributions from group 23 to outgoing groups 18 - 25. In Figures 4a and 4b (which plot downscattered angular distributions), we observe that the Legendre moment treatment fails to capture even the rough angular shape of the CSK. While the PDF in Figure 3 suggests that the ze-

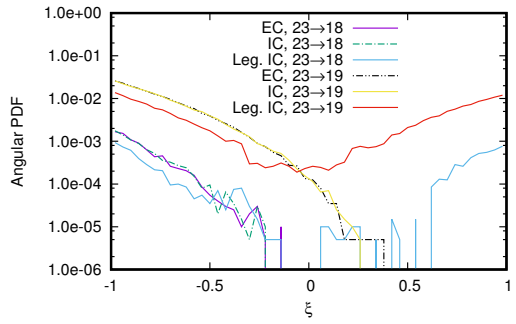

(a) $g' = 18$-19

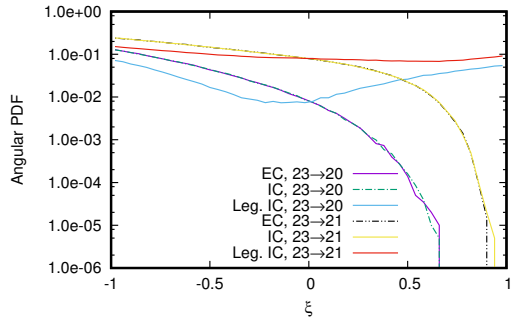

(b) $g' = 20$-21

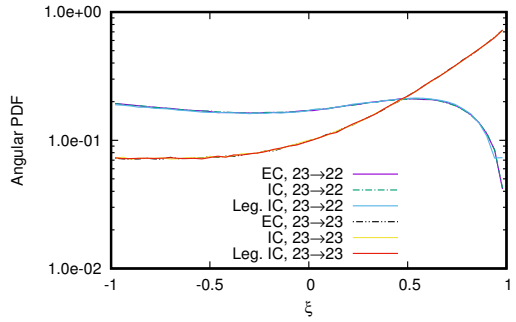

(c) $g' = 22$-23

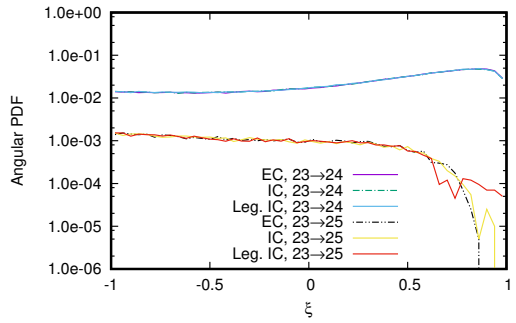

(d) $g' = 24$-25

Fig. 4. Single-scatter angular (ξ) distribution functions for $g = 23$.

roth IC Legendre moment accurately represents the integral of the CSK over ξ, the full P_{50} shape function clearly allows photons to scatter in impossible directions for certain group-to-group combinations. For the case presented here, this is most prevalent in the downscattered groups (where the CSK is nearly zero over a large fraction of the angular domain). Angular distributions for the inscatter and upscatter groups are largely smooth, slowly-varying functions of ξ, and can thus be accurately approximated by Legendre polynomials.

By contrast, the IC method with explicit angular treatment accurately recreates the EC shape function for all group-to-group combinations shown in Figure 4. Because the Legendre and explicit multigroup IC libraries are formed from the same pointwise CSK library, inaccuracies in the Legendre treatment are almost certainly due to the inability of the polynomial approximation to capture steep variation in the CSK (rather than an error in the Legendre moment calculation).

2. Planck-weighted multigroup library

In this section, we consider a Planck-weighted twenty-group library spanning from $\nu_0 = 0.55$ keV to $\nu_{max} = 10.5$ keV. The lowest frequency group has width $\Delta\nu = 0.45$ keV, while all other groups have width $\Delta\nu = 0.5$ keV. Radiation and matter are assumed to be at equilibrium, such that $T_m = T_r \approx 0.345$ keV. To maintain a fair comparison between EC and IC, we only tally EC scatters which take place fully within the group structure of the IC library. As in the flat-weighted case, we simulate 5e6 total scattering events; however, here the intial particle frequency is sampled from a Planckian at the material temperature (in keeping with the spectral weighting function of the library).

We will compare results for two Planck-weighted libraries generated using the same twenty-group structure, each based on a different underlying pointwise library. This allows us to expose some of the systematic error in the IC treatment (and show that it decreases as the pointwise interpolation library is refined). We will refer to these two libraries as the "coarse" and "fine" Planck-weighted libraries, reflecting the number of interpolation regions in the underlying pointwise data. Both of the Planck-weighted libraries use an explicit angular treatment, with 200 evaluation points in ξ.

In Section III.2.A., we present and compare distribution functions in angle and frequency group. We then move to average outgoing frequency distributions in Section III.2.B., which show that use of the new multigroup IC method can significantly smooth outgoing frequency curves for Compton events (relative to the existing EC method).

A. Angle and outgoing group distributions

We begin by comparing differences in single-scattering group-to-group PDFs for the coarse and fine Planck-weighted IC libraries, relative to EC results. These are plotted in Figure 5 using a group-to-group heatmap. In general, the in-group IC scattering opacities show close agreement with the EC values, with relative differences ranging from tenths of a percent for the lower groups to several percent for the higher groups. The immediate off-diagonal scattering probabilities appear to be less accurate, with maximum differences of roughly 15% for the coarse library and 10% for the fine library. Large relative error is observed in the outer off-diagonal values, which tend to be very small in absolute magnitude ($O(10^{-6})$ or less). As discussed in Section II.2.A., the Lagrange interpolation method becomes very inaccurate when the CSK drops near zero, sometimes producing negative or oscillating opacity values; thus, the observed increase in error in this regime is not surprising.

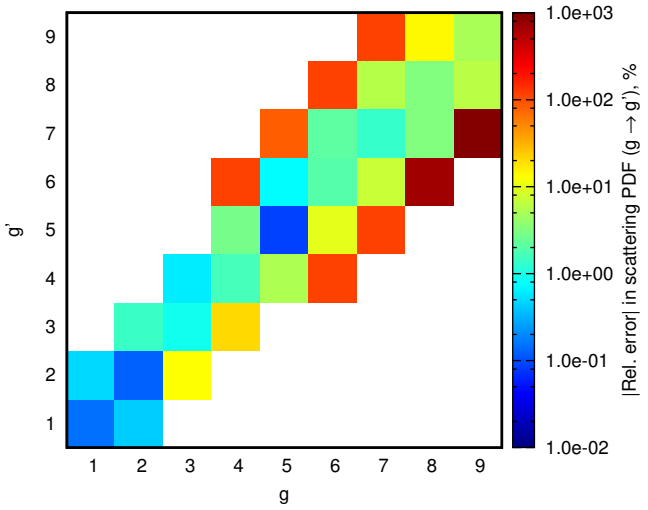

(a) Coarse IC

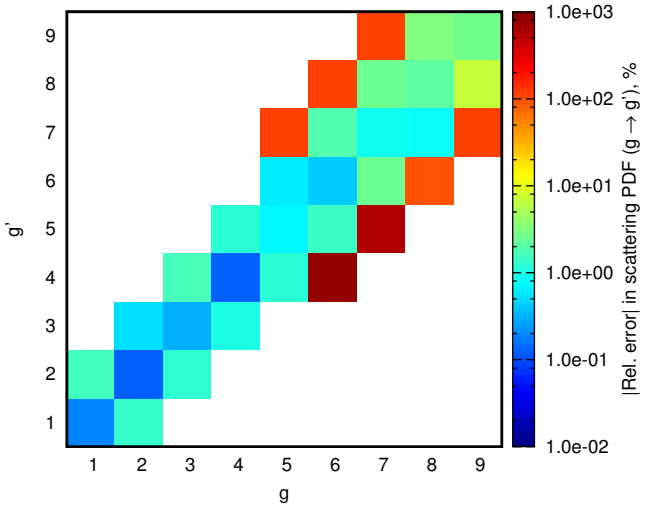

(b) Fine IC

Fig. 5. Relative difference in single-scatter group-to-group distributions (versus EC values)

As expected, group-to-group scattering probabilities for the fine Planck-weighted IC library generally agree with the EC values more closely than the coarse IC library values do (with the exception of a few values).

Figure 6 presents scattering angle distributions for photons originating in frequency group 4 of the Planck-weighted libraries. These plots show close agreement between all three ξ-distribution curves, which indicates that the coarser IC li-

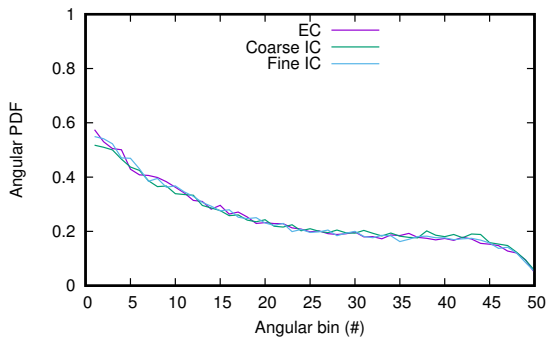

(a) Group 4→3

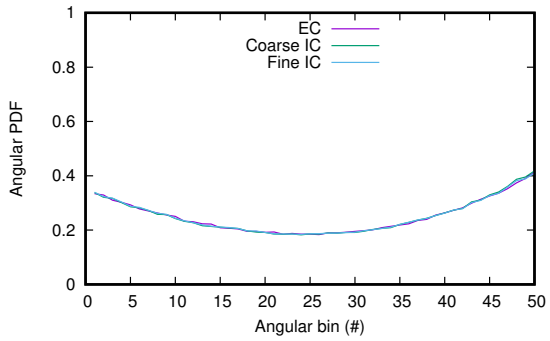

(b) Group 4→4

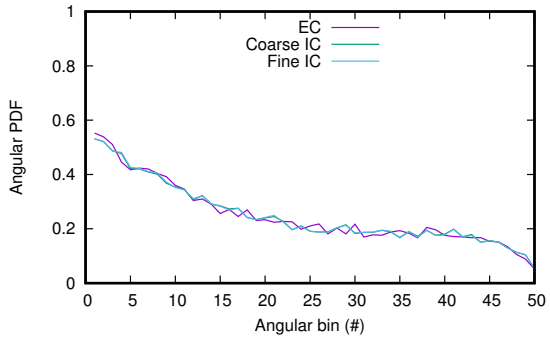

(c) Group 4→5

Fig. 6. Angular PDFs for group 4

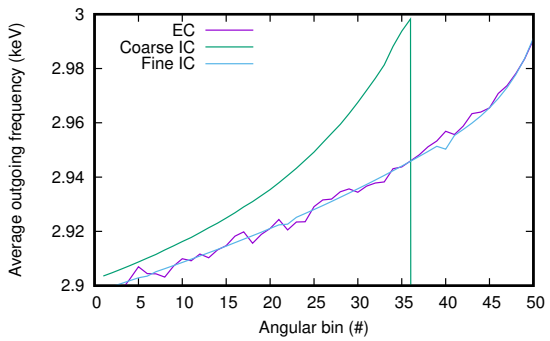

(a) Group 6→5

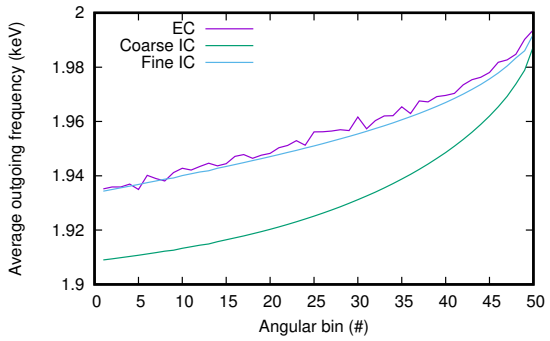

(b) Group 4→3

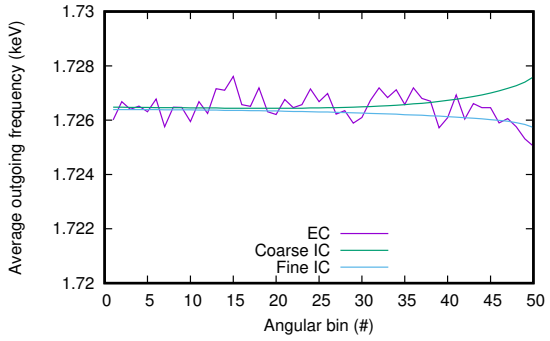

(c) Group 3→3

Fig. 7. Average outgoing frequency distributions, select $g \rightarrow g'$ combinations

brary is sufficient to resolve the angular shape of the CSK for the cases shown here.

B. Outgoing frequency distributions

In this section, we compare outgoing frequency distributions for the EC and IC methods. These results are especially relevant to our ultimate goal, which is to decrease statistical noise from Compton events in IMC material energy deposition tallies.

As described in Section II.2., the outgoing frequency of photons scattered via the IC method is determined using both the sampled outgoing frequency group and angular bin (the average outgoing frequency having been calculated and stored for each $(g \rightarrow g', l)$ data point when the multigroup library was constructed). This approach resolves the photon frequency spectrum more fully than sampling the photon frequency uniformly within the outgoing group, which in turn ensures an accurate energy deposition distribution. If further research indicates that this level of spectral resolution is unnecessary, existing $\bar{\gamma}^{l}_{g\rightarrow g'}$ data can be averaged over angle to yield a single value for each $g \rightarrow g'$ combination; this method should still be more accurate than assuming a uniform distribution across the outgoing group.

First, we consider average outgoing photon frequency as a function of incoming/outgoing group, averaged over all scattering bins. We observe that the average outgoing frequency is rarely near the center of the outgoing frequency bin, which supports our use of a numerically-estimated $\bar{\gamma'}^{l}_{g\rightarrow g'}$ (as described in Section II.2.). We note that the frequency results presented in this section are reported in keV; that is, the

TABLE I. Average outgoing frequency ($\bar{\nu}'$, given in keV) and relative difference with respect to EC, selected $g \rightarrow g'$ combinations. (Relative differences > 0.1% in magnitude are highlighted in red.)

g	g'	$\bar{\nu}'_{g\rightarrow g',\,EC}$	$\bar{\nu}'_{g\rightarrow g',\,IC}$ (coarse)	% diff. (coarse)	$\bar{\nu}'_{g\rightarrow g',\,IC}$ (fine)	% diff. (fine)
1	1	0.782493	0.782082	-0.0525786	0.782336	-0.0200912
1	2	1.02536	1.02531	-0.0055943	1.02537	0.000273598
2	1	0.975947	0.975883	-0.00650749	0.975491	-0.0467178
2	2	1.23661	1.23719	0.0469461	1.23662	0.000283706
2	3	1.53723	1.5374	0.0110295	1.53737	0.00904381
3	2	1.46322	1.47597	0.871292	1.46475	0.104377
3	3	1.72628	1.72666	0.0219108	1.72622	-0.00328709
3	4	2.04916	2.04906	-0.00504176	2.04906	-0.00483141
4	3	1.95051	1.92507	-1.30403	1.94855	-0.100211
4	4	2.22098	2.22016	-0.0368092	2.22097	-0.000409172
4	5	2.56084	2.56013	-0.0275214	2.5602	-0.0248179
5	4	2.43618	2.42633	-0.404124	2.43731	0.0464823
5	5	2.71829	2.718	-0.0106635	2.71828	-0.000554672
5	6	3.06979	3.07082	0.0335122	3.07081	0.0331922
6	5	2.92323	2.92825	0.171718	2.92254	-0.0233587
6	6	3.21645	3.21347	-0.0923754	3.21676	0.00992572
6	7	3.5818	3.58118	-0.0175653	3.58109	-0.020091

unitless frequency variable has been multiplied by the electron rest-mass to yield a more physically-relevant quantity:

$$\bar{\nu}'_{g\rightarrow g'} = m_e \bar{\gamma}'_{g\rightarrow g'} \ .$$

The data in Table I reveals very close agreement between EC and fine IC $\bar{\nu}'_{g\rightarrow g'}$ estimates, with a maximum relative difference of roughly 0.1% for the group-to-group combinations shown here. The coarse averages are less accurate, with a maximum relative difference of well over 1.0%. While differences on the order of a percent may seem trivial, we stress that said differences are measured *per scattering event*; these small systematic biases can compound in problems where delicate energy deposition cancellations occur between inverse and regular Compton events.

Finally, in Figure 7 we examine average outgoing frequency distributions in angle for select $g \rightarrow g'$ combinations. Figures 7a and 7b were chosen because they represent cases where the coarse IC $\bar{\nu}'_{g\rightarrow g'}$ estimate in Table I differs significantly from the EC value. In these cases, the coarse IC $\bar{\nu}'^{l}_{g\rightarrow g'}$ distributions deviate significantly from the corresponding EC curves. When the fine multigroup IC library is used instead, the same $\bar{\nu}'^{l}_{g\rightarrow g'}$ curves show good agreement with the EC data. Thus, these figures support the idea that systematic error in multigroup IC simulations can be mitigated by regenerating the underlying pointwise library with higher frequency resolution. Figure 7c illustrates the smooth nature of the IC $\bar{\nu}'^{l}_{g\rightarrow g'}$ curves when compared to the EC data.

We summarize our Planck-weighted results by stressing that the equilibrium case presented in this section is a particularly strenuous test of the IC method. Because radiation and matter are fully equilibrated, there should be zero net energy deposition from radiation to matter (in the infinite-particle limit). In order for our multigroup library to replicate this result, delicate numerical cancellations must occur between regular and inverse Compton events. This requires that the group-to-group scattering probabilities, angular distributions, and average outgoing frequencies all be highly accurate. While our current libraries produce excellent angular distributions and average outgoing energy estimates, enough systematic error exists in the group-to-group scattering probabilities to skew energy deposition slightly.

IV. CONCLUSIONS AND FUTURE WORK

Compton scattering is difficult to model accurately and efficiently with IMC, especially when the kinetic energy of the colliding electron is non-negligible. Because the CSK depends strongly on four independent variables, attempts to sample it explicitly increase noise in energy deposition tallies, which in turn increases variance in material temperature updates. This additional variance is especially problematic when the coupled to other physics, such as hydrodynamics.

In this research, we have developed an alternative to explicit Monte Carlo CSK sampling. Our approach involves interpolating between electron temperature evaluation points in a multigroup data library to obtain discrete probability distributions for outgoing frequency and angle. Preliminary results indicate that this method is capable of accurately modeling Compton scattering; however, great care must be taken to ensure that the pointwise library is resolved enough to produce accurate group-to-group scattering opacities. To this end, we plan to undertake a parametric study to optimize our pointwise library discretization over as large a range of input parameters as feasible.

As hypothesized in Section II., the direct sampling procedure used by IC is more efficient than the rejection sampling required by the EC method, averaging ~60-80% of the com-

putation time per scatter; however, it is difficult to predict whether the IC method will reduce total simulation time for a particular problem, because the multigroup opacities must be interpolated in electron temperature for each spatial cell at each timestep.

To date, we have developed and implemented an interpolation method which is capable of capturing CSK boundary layers in electron temperature and frequency. However, the proposed Legendre moment treatment in angle will likely be insufficient for problems with significant angular dependence. As a result, we currently construct our PDF in ξ using explicit CSK evaluations. While this is an acceptable treatment for IMC, it is not easily extended to discrete-ordinates simulations. Because we ultimately desire a data library that can be called directly by either IMC or discrete-ordinates codes, further research is needed.

The existing IC method decreases statistical noise in the post-scatter photon frequency spectrum, relative to the EC method. In the future, a priori knowledge of the scattering distribution will enable us to test a number of additional variance-reduction techniques. For example, we can choose to sample multiple outgoing photons for each scatter, such that the net energy deposition is less noisy than the explicit treatment. Alternatively, we can further simplify the outgoing energy and/or angular distributions using methods described previously (while preserving essential features of the CSK).

Finally, the Lagrange polynomial method used to handle frequency in/out interpolation can produce unphysical negative scattering opacities from non-negative input data. While this behavior can be minimized by increasing the number of breakpoint regions and/or local interpolation points per region, it cannot be eliminated entirely. Thus, it may prove beneficial to adopt a strictly-positive interpolation method in frequency space.

ACKNOWLEDGMENTS

This work was performed under U.S. government contract DE-AC52-06NA25396 for Los Alamos National Laboratory, which is operated by Los Alamos National Security, LLC, for the U.S. Department of Energy.

REFERENCES

1. D. S. KERSHAW, M. K. PRASAD, and J. D. BEASON, "A Simple and Fast Method for Computing the Relativistic Compton Scattering Kernel For Radiative Transfer," J. Quant. Spectrosc. Radiat. Transfer, 36, 4, 273-282 (1985).

2. E. CANFIELD, W. M. HOWARD, and E. P. LIANG, "Inverse Comptonization by One-Dimensional Relativistic Electrons," Astrophysical Journal, 323, 565-574 (1987).